Energetic Ion Effects on the Ion Saturation Current *

Bin-Bin Lin(林滨滨)[1,2**], Nong Xiang(项农)[1,2**], Jing Ou(欧靖)[1,2], Xiao-Yun Zhao(赵晓云)[1,2,3]

[1]*Institute of Plasma Physics, Chinese Academy of Sciences, Hefei 230031*
[2]*Center for Magnetic Fusion Theory, Chinese Academy of Sciences, Hefei 230031*
[3]*School of Physics and Electronic Engineering, Fuyang Normal University, Fuyang 236037*

(Received 24 October 2016)

The ion saturation current is very important in probe theory, which can be used to measure the electron temperature and the floating potential. In this work, the effects of energetic ions on the ion saturation current are studied via particle-in-cell simulations. It is found that the energetic ions and background ions can be treated separately as different species, and they satisfy their individual Bohm criterion at the sheath edge. It is shown that the energetic ions can significantly affect the ion saturation current if their concentration is greater than $\sqrt{T_e/(\gamma_{i2}T_{i2})}$*, where* T_e *is the electron temperature, and* γ_{i2} *and* T_{i2} *represent the polytropic coefficient and temperature of energetic ions, respectively. As a result, the floating potential and the I–V characteristic profile are strongly influenced by the energetic ions. When the energetic ion current dominates the ion saturation current, an analysis of the ion saturation current will yield the energetic ion temperature rather than the electron temperature.*

PACS: 52.40.Kh, 52.65.Rr, 52.27.Cm DOI: 10.1088/0256-307X/34/1/015203

Langmuir probes are often used as plasma diagnostics in fusion experiments due to their apparent simplicity to determine the plasma temperature and floating potential. The current collected by the probe consists of the ion and electron currents from the plasma. When the bias voltage on the probe is sufficiently negative with respect to the plasma potential, the probe collects the ion saturation current.[1] The ion saturation current density can be expressed as $J_{is} = en_iV_B$, where $V_B = \sqrt{k(T_e + \gamma_i T_i)/m_i}$ is the Bohm velocity, e is the elementary charge, n_i is the ion density, k is the Boltzmann constant, m_i is the ion mass, T_i is the ion temperature, and γ_i represents the ion polytropic coefficient. In the classical probe theory considering a plasma where $T_e \sim T_i$, the assumption $\gamma_i = 1$ is employed. As long as the ion density is obtained, the electron temperature can be easily found from the ion saturation current density. Also, a multi-fluid model has shown that raising the ion polytropic coefficient increases the ion saturation current.[2]

The sheath may contain energetic particles which come from, for example, the wave heating or non-inductive current drive.[3,4] Many studies have been carried out for the sheath formation in a plasma containing high-energy electron beams.[5,6] However, the energetic ion effects on the ion saturation current have received only slight attention so far. The presence of energetic ions may make a significant contribution to the ion saturation current, indicating that the classical probe theory which excludes the energetic ion effect will lead to inaccurate measurements of the plasma temperature and floating potential.

In this work, the sheath containing energetic ions is studied via the particle-in-cell (PIC) simulation. To evaluate the energetic ion effects, energetic ions are now treated as another ion species different from the background cold ions. Thus the Bohm criterion can be expressed as[7]

$$\sum_i \frac{e_i^2 n_i}{m_i} \langle v_x^{-2} \rangle_i \leq \frac{e^2 n_e}{kT_e}, \tag{1}$$

where the sum is over the number of ion species, the brackets $\langle\rangle_i$ denote an average with the velocity distribution function (VDF) of the ion component, e_i is the charge of ion, v_x is the component of ion velocity perpendicular to the wall, and n_e is the electron density. The equality of Eq. (1) is usually assumed to determine the sheath edge.

The hierarchy chain of hydrodynamic equations derived from the kinetic equation must be cut by some *ad hoc* assumptions. A widely used approach is to express the ion pressure gradient term in the ion momentum equation as

$$\nabla p_i = \gamma_i k T_i \nabla n_i, \tag{2}$$

where p_i is the ion pressure. When the ansatz Eq. (2) is valid, Eq. (1) can be simply expressed as[7]

$$\sum_i \frac{e_i^2 n_i}{m_i u_i^2 - \gamma_i k T_i} \leq \frac{e^2 n_e}{kT_e}, \tag{3}$$

where u_i is the ion drift velocity. For a collisionless plasma, it is confirmed from many models that each ion species satisfies its individual Bohm criterion in the absence of two-ion streaming instability.[8–11]

*Supported by the Program of Fusion Reactor Physics and Digital Tokamak with the Chinese Academy of Sciences 'One-Three-Five' Strategic Planning, the JSPS-NRF-NSFC A3 Foresight Program in the Field of Plasma Physics (NSFC No 11261140328 and NRF No 2012K2A2A6000443), the National ITER Program of China under Grant No 2015GB101003, and the National Natural Science Foundation of China under Grant Nos 11405215, 11475223 and 11505236.

**Corresponding author. Email: linbinbin@ipp.ac.cn; xiangn@ipp.ac.cn

© 2017 Chinese Physical Society and IOP Publishing Ltd

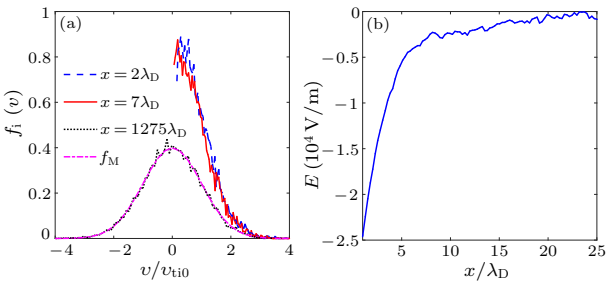

Fig. 1. (a) Energetic ion velocity distributions in the bulk plasma (black dotted line, $x = 1275\lambda_D$), in the vicinity of the sheath edge (red solid line, $x = 7\lambda_D$), in the sheath region (blue dashed line, $x = 2\lambda_D$) and (b) spatial variation of the electric field for the case of $C_h = 0.1$. The magenta dashed-dotted line represents the Maxwellian distribution function f_M. Here v_{ti0} denotes the thermal velocity of ions in the bulk plasma.

To check the validity of ansatz Eq. (2) for the energetic ions, the simulations are conducted by using the plasma simulation code VSIM of Tech-X corporation originated from PIC code VORPAL.[12] The simulation domain of our model is one-dimensional in configuration space and three-dimensional in velocity space. The Vlasov equation together with Maxwell's equations is solved. The spatially homogeneous plasma with the density equal to $10^{16}\,\mathrm{m}^{-3}$ is initially loaded between two perfect conducting electrodes separated with a distance $L = 0.6\,\mathrm{m}$. The absorbing boundary condition is used at $x = 0$ and 0.6 m so that the particles will be removed out of the system when reaching the walls. Thus there will be one sheath near each wall while the results shown in our study are between $x = 0$ and $L/2$. The positive direction of the ion velocity is towards the wall ($x = 0$). The loaded superparticles consist of Maxwellian ions and electrons. The simulations are conducted to study the sheath which consists of electron and two-temperature ion components with the initial temperatures as: $T_{e0} = 10\,\mathrm{eV}$, $T_{i10} = 10\,\mathrm{eV}$, $T_{i20} = 1\,\mathrm{keV}$. With these parameters $L/\lambda_D \approx 2550 \gg 1$, where λ_D is the Debye length. The mean free path of background ions is estimated to be 35 m, which is much larger than the simulation domain size L, indicating that the collisionless sheath model is suitable for the modeling of the Langmuir probe. Also, particle source is excluded in the simulations. As the plasma length is much greater than the Debye length, the ion transit time ($L/v_{ti} \sim 10^{-6}\,\mathrm{s}$, where v_{ti} denotes the ion thermal velocity) from the center to both walls is much longer than the timescale of sheath formation ($\lambda_D/V_B \sim 10^{-8}\,\mathrm{s}$). Therefore, the bulk plasma acts like a source for the sheaths, and the plasma parameters in the core region, such as the density and temperature, change slightly during the sheath formation. It is nature that if the energetic ion temperature increases, the simulation domain needs to be larger to ensure that the bulk plasma still acts like a source. To save the computational expense, we take $T_{i20} = 1\,\mathrm{keV}$ to represent the temperature of energetic ions. To resolve the sheath, we take the grid size as $6 \times 10^{-5}\,\mathrm{m}$, which is about 1/4 of the Debye length. The numbers of superparticles for the electrons and ions in the system are both nearly 3.6×10^7.

The validity of ansatz Eq. (2) is confirmed in the sheath containing hot ions as $T_{i20} \leq 200\,\mathrm{eV}$ in our previous work,[13] while this validity remains to be examined for energetic ions. It is well known that the kinetic effects of ions increase with the ion temperature. To show the kinetic effects, Fig. 1(a) plots the ion velocity distribution functions at different positions for $C_h = 0.1$. Here $C_h = n_{i2}/(n_{i1} + n_{i2})$ represents the energetic ion concentration, where n_{i1} and n_{i2} denote the densities of background and energetic ions, respectively. Apparently, the VDF is Maxwellian in the bulk plasma while the VDFs in the sheath are non-Maxwellian. As the electric field may play an important role in the evolution of VDFs, we plot the spatial variation of electric field as shown in Fig. 1(b). One can see that the electric field is strong in the sheath, and becomes weaker outside the sheath, i.e., the presheath region. Due to the ion acceleration in the presheath, the ions with negative velocity disappear. The ion VDFs evolve distinctly under different electric fields, which is similar to Ref. [14]. In our previous work, the width of the VDF becomes narrower towards the wall due to the electric field for the sheath containing hot ions.[13] Different from this, for the sheath containing energetic ions, the VDF near the wall is almost the same as that in the vicinity of the sheath edge because the energetic ion energy is much larger than the potential energy in the sheath.

We calculate γ_i from its definition Eq. (2), which is equivalent to[15,16]

$$\gamma_i(r,t) \equiv 1 + \frac{n_i}{T_i}\frac{dT_i}{dn_i}. \tag{4}$$

Using the VDFs from the simulations, the ion density and temperature profiles are obtained with the standard definitions for the average moment quantities $n_i = \int f_i(v)dv$, $u_i = \int v f_i(v)dv/n_i$, and $T_i = [\int m_i(v-u_i)^2 f_i(v)dv]/n_i$, where f_i is the ion velocity distribution function. As the ion velocity distribution is non-Maxwellian[17,18] in the sheath, the effective temperature can be obtained. As the energetic ion concentration (C_h) varies, the ion polytropic coefficients of energetic ions (γ_{i2}) are shown in Fig. 2. Equation (1) is employed to locate the plasma-sheath interface. It is found that γ_{i2} is indeed nearly a constant in the vicinity of the sheath edge. As C_h varies, γ_{i2} is between 1.4–1.6. The fact that γ_{i2} is nearly a constant implies that the ansatz Eq. (2) may still exist to close the hierarchy of fluid equations with an appropriate polytropic coefficient. The obtained ion polytropic coefficients are different from those in Refs. [15,16,19]. It is shown that for a sheath with a cold ion source, γ_i can take a wide range of local values in the plasma-sheath transition region and has a sharp kink at the sheath edge.[16] Different from this, we find that γ_i can be nearly constant in the vicinity of the sheath edge in the model excluding particle sources and collisions.[13]

Because the kinetic effects of ions increase with the ion temperature, the heat flux can significantly affect the energy equation, leading to the deviation of γ_i from 3 (corresponding to one-dimensional adiabatic flow). Such a difference may be due to the dimensionality, the absence of collisions and particle sources.

With the modified polytropic coefficient, the ions can be described by the fluid model, and satisfy the fluid Bohm criterion Eq. (3). Figure 3 plots the spatial variations of the ion drift velocities normalized to their individual modified Bohm velocities. Here $V_{B1} = \sqrt{k(T_e + \gamma_{i1}T_{i1})/m_i}$ and $V_{B2} = \sqrt{k(T_e + \gamma_{i2}T_{i2})/m_i}$ represent the Bohm velocities of background and energetic ions at the sheath edge, and u_{i1} and u_{i2} are their individual drift velocities, respectively. One can see that with the ion polytropic coefficients obtained from the simulation results, the Bohm criterion is nearly satisfied at the sheath edge.

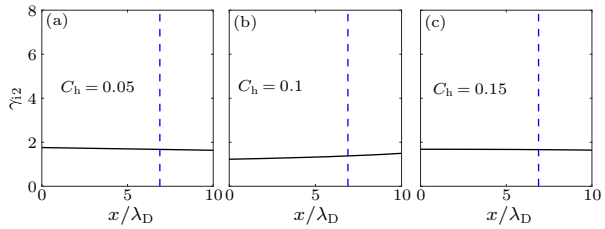

Fig. 2. Spatial variation of the polytropic coefficients for different C_h, (a) $C_h = 0.05$, (b) $C_h = 0.1$, and (c) $C_h = 0.15$. The vertical blue dashed line represents the sheath edge.

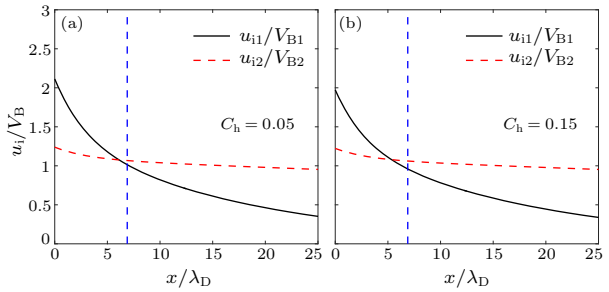

Fig. 3. Spatial variations of the ion drift velocities normalized to the Bohm velocities, for different energetic ion concentrations, (a) $C_h = 0.05$, and (b) $C_h = 0.15$. Black solid lines denote the background ions, and red dotted lines denote the energetic ions.

As the ions enter the sheath at their individual Bohm velocities, the ion saturation current density can be expressed as $J_{is} = J_{eng} + J_{bg}$, where $J_{eng} \approx eC_h n_0 \sqrt{k\gamma_{i2}T_{i2}/m_i}$ is the energetic ion current density, $J_{bg} \approx e(1-C_h)n_0\sqrt{k(T_e + \gamma_{i1}T_{i1})/m_i}$ is the background ion current density, and $n_0 = n_{i1} + n_{i2}$ represents the plasma density at the sheath edge. If the contribution of energetic ion to the ion saturation current is excluded, the analysis of ion saturation current density will yield an electron temperature $((1-C_h)/(1-J_{eng}/J_{is}))^2$ times larger than its real value. As $T_{i2} \gg T_e$, if $C_h \sim \sqrt{T_e/(\gamma_{i2}T_{i2})}$, J_{eng} would be comparable to J_{bg}. This indicates that the ion saturation current density may be affected even for a small C_h. Under this condition, the obtained electron temperature may be four times larger than its real value, and this error will increase with J_{eng}/J_{is}.

Table 1. Calculated J_{eng}/J_{is} for different C_h at the sheath edge.

C_h	0.05	0.1	0.15
J_{eng}/J_{is}	0.27	0.45	0.56

As discussed above, the ion saturation current density strongly depends on C_h. To illustrate this dependence, J_{eng}/J_{is} are calculated by using the simulation results for different C_h as listed in Table 1. Due to the energy transport in the sheath, the temperatures of electrons and ions decrease compared with their initial values. Typically, $T_e \approx 8.5$ eV, $T_{i1} \approx 2.8$ eV, $T_{i2} \approx 354$ eV at the sheath edge when the steady state is reached in our simulations. The energetic ion concentration is almost equal to its initial value at the sheath edge. One can see that the energetic ion current density increases with C_h. The results suggest that the ion saturation current density may be significantly affected in the presence of energetic ions though C_h is very small.

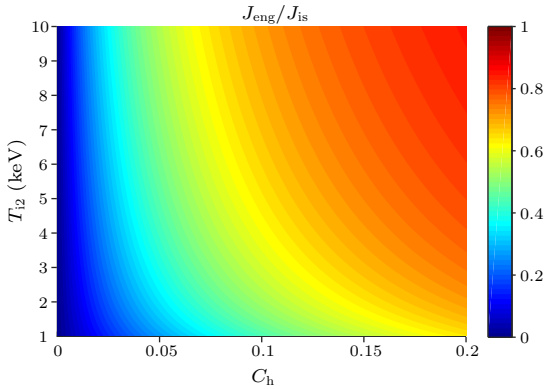

Fig. 4. Dependence of J_{eng}/J_{is} on the energetic ion temperature and concentration.

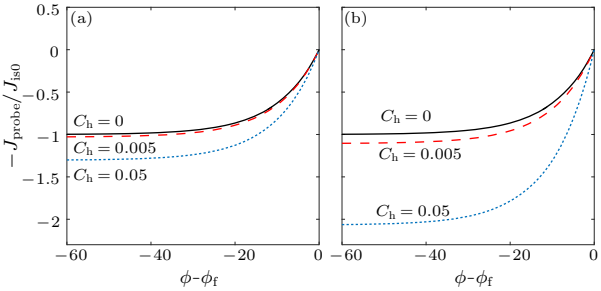

Fig. 5. The I–V characteristic for different energetic ion temperatures, (a) $T_{i2} = 1$ keV and (b) $T_{i2} = 10$ keV. Black solid lines denote the I–V characteristic profiles without energetic ions, and red dashed lines and blue dotted lines denote the I–V characteristic profiles for $C_h = 0.005$ and $C_h = 0.05$, respectively.

In fusion plasma, the energetic ion energy may be up to a few tens of keV. In this case, the energetic ions may be dominant in the measured ion saturation current even for a very small C_h. Figure 4 plots J_{eng}/J_{is}

as a function of energetic ion temperature and concentration. For example, as the energetic ion energy exceeds 20 keV,[20] for $C_h \sim 0.1$, $J_{eng}/J_{is} \sim 0.86$, J_{eng} would dominate the ion saturation current density. As a result, the measured ion saturation current will yield the energetic ion temperature rather than the electron temperature. On the other hand, as the fraction of ion saturation current contributed by energetic ions is significant, the floating potential can also be affected. This can be seen from the expression $\phi_f = kT_e \ln(J_{is}/(en_0u_e))/e$, where ϕ_f is the floating potential, and u_e is the electron average velocity at the wall. We can construct the I–V probe characteristic through[6] $J_{probe} = J_{is} - J_e$, where J_{probe} is the current density collected by the probe, and $J_e = en_0 \exp(e\phi/kT_e)u_e$ is the electron current density as a function of the bias potential ϕ. Figure 5 plots the I–V characteristic profiles for different energetic ion temperatures and concentrations. Here J_{probe} is normalized by J_{is0}, which is the ion saturation current density when $C_h = 0$. As is expected, the I–V characteristic is significantly affected by C_h. Even for a small energetic ion concentration $C_h = 0.05$, the difference between the I–V characteristic profiles can be 30% for $T_{i2} = 1$ keV and 107% for $T_{i2} = 10$ keV.

In summary, the sheath in the presence of energetic ions has been studied via PIC simulations. The ansatz Eq. (2) is confirmed to be valid for truncation of the hierarchy chain of hydrodynamic equations as the ion polytropic coefficient is found to be nearly a constant in the vicinity of the sheath edge. For the sheath containing energetic ions, the ions enter the sheath at their individual Bohm velocities as C_h varies. Therefore, the ion saturation current density is a combination of the energetic and background ion current density. The analytical result shows that the ion saturation current density can be significantly affected by the energetic ions though C_h is very small as $C_h \sim \sqrt{T_e/(\gamma_{i2}T_{i2})}$, which is confirmed by the simulation results. As a result, the measured ion saturation current can no longer determine the electron temperature, and the I–V characteristic profile is significantly affected by the energetic ions. It is expected that the conclusions can be applied for the sheath containing different ion species, e.g., the deuterium plasmas featuring hydrogen minority or the plasmas containing energetic alpha particles. In this work, the model excluding the particle sources and collisions shows that γ_{i2} is nearly constant in the vicinity of the sheath edge in the sheath containing energetic ions. Some questions such as the validity of ansatz Eq. (2) in the sheath with an oblique magnetic field, and the multi-dimensional effect on the variation of γ_i remain to be studied. The ion saturation current remains to be investigated in the sheath containing both energetic ions and electrons for the future work.

References

[1] Merlino R L 2007 *Am. J. Phys.* **75** 1078
[2] Khoramabadi M and Masoudi S F 2013 *Chin. Phys. Lett.* **30** 085202
[3] Heidbrink W W and Sadler G J 1994 *Nucl. Fusion* **34** 535
[4] Zhu Y B, Heidbrink W W and Pickering L D 2010 *Nucl. Fusion* **50** 084024
[5] Stangeby P C 1995 *Plasma Phys. Control. Fusion* **37** 1031
[6] Ou J, Lin B B, Zhao X Y and Yang Y L 2016 *Plasma Phys. Control. Fusion* **58** 075004
[7] Riemann K U 1995 *IEEE Trans. Plasma Sci.* **23** 709
[8] Hatami M M, Niknam A R, Shokri B and Ghomi H 2008 *Phys. Plasmas* **15** 053508
[9] Xiang N, Hu Y M and Ou J 2011 *Plasma Sci. Technol.* **13** 385
[10] Franklin R N 2003 *J. Phys.* D **36** 1806
[11] Zhao X Y, Xiang N, Ou J, Li D H and Lin B B 2016 *Chin. Phys.* B **25** 025202
[12] Nieter C and Cary J R 2004 *J. Comput. Phys.* **196** 448
[13] Lin B B, Xiang N and Ou J 2016 *Phys. Plasmas* **23** 083508
[14] Weng S M, Sheng Z M, He M Q, Zhang J, Norreys P A, Sherlock M and Robinson A P 2008 *Phys. Rev. Lett.* **100** 185001
[15] Teodoru S, Tskhakaya D, Kuhn S, Tskhakaya D D, Schrittwieser R, Ionita C and Popa G 2005 *J. Nucl. Mater.* **337** 1111
[16] Kuhn S, Riemann K U, Jelicí N, Tskhakaya D D, Tskhakaya D and Stanojevicí M 2006 *Phys. Plasmas* **13** 013503
[17] Stangeby P C 2000 *The Plasma Boundary of Magnetic Fusion Devices* (Bristol: IOP)
[18] Devaux S and Manfredi G 2006 *Phys. Plasmas* **13** 083504
[19] Jelicí N, Riemann K U, Gyergyek T, Kuhn S, Stanojevicí M and Duhovnik J 2007 *Phys. Plasmas* **14** 103506
[20] Pace D C, Pinsker R I, Heidbrink W W, Fisher R K, Van Zeeland M A, Austin M E, McKee G R and Garcia-Munoz M 2012 *Nucl. Fusion* **52** 063019